

Suppression of the $\gamma - \alpha$ structural phase transition in $\text{Ce}_{0.8}\text{La}_{0.1}\text{Th}_{0.1}$ by large magnetic fields

F. Drymiotis¹, J. Singleton¹, N. Harrison¹, L. Balicas², A. Bangura³,
C.H. Mielke¹, Z. Fisk⁴, A. Migliori¹, J.L. Smith¹ and J.C. Lashley¹

¹*Los Alamos National Laboratory, Los Alamos, NM87545, USA*

²*National High Magnetic Field Laboratory, 1800 E. Paul Dirac Drive, Tallahassee, FL32310, USA*

³*Condensed Matter Physics, Department of Physics,
University of Oxford, The Clarendon Laboratory,
Parks Road, Oxford OX1 3PU, United Kingdom*

⁴*Department of Physics, University of California, Davis, CA95616, USA*

The $\gamma - \alpha$ transition in $\text{Ce}_{0.8}\text{La}_{0.1}\text{Th}_{0.1}$ is measured as a function of applied magnetic field using both resistivity and magnetization. The $\gamma - \alpha$ transition temperature decreases with increasing magnetic field, reaching zero temperature at around 56 T. The magnetic-field dependence of the transition temperature may be fitted using a model that invokes the field and temperature dependence of the entropy of the $4f$ -electron moments of the γ phase, suggesting that the volume collapse in Ce and its alloys is primarily driven by entropic considerations.

PACS numbers: 75.20.Hr, 71.20.Ps, 71.27.-a

The element Ce has attracted considerable theoretical and experimental interest over the past fifty years (see *e.g.* Refs. [1, 2, 3, 4, 5, 6] and references therein). One of the most fascinating aspects of its behavior is the 14.8 % collapse in volume that occurs when the face-centred-cubic (fcc) γ phase transforms into the fcc α phase on cooling through $T_{\gamma\alpha} \approx 100$ K at ambient pressure [2, 5, 6]. Although it is generally accepted that this isostructural volume collapse is caused by the Ce $4f$ electrons, a variety of models invoking different physical mechanisms have been proposed. For example, the *Mott transition model* proposes that the $4f$ electrons behave as simple band electrons in the α phase but are localized on the Ce ions in the γ phase [6, 7, 8, 9]. This approach [7] accounts qualitatively for the reduction in magnetic susceptibility χ that accompanies the volume collapse [2, 10]. However, such a picture is certainly an over-simplification. Neutron scattering [11] and other experiments (see Refs. [12, 13, 14] and citations therein) suggest a large $4f$ -electron spectral weight on the Ce site in the α phase. This observation has been interpreted as evidence for “localized” f electrons [5, 11]; however, a Ce occupancy of 0.8 ± 0.1 could also be consistent with itinerant f electrons within a narrow-band, tight-binding picture.

The alternative *Kondo volume collapse model* proposes that both the α and γ phases possess highly-correlated $4f$ electrons, but with very different effective Kondo temperatures [5, 11, 12, 13]. In this scheme, the effective Kondo temperature of the γ phase is small, (*i.e.* less than $T_{\gamma\alpha}$); in the γ phase the properties of the $4f$ electrons will therefore be almost indistinguishable from those of localized ionic moments. It is thought that the α phase has a relatively large effective Kondo temperature by comparison [11, 14], causing the $4f$ electrons to be in the mixed-valence regime with significant *spd* and *f* hybridization at low temperatures. Consequently one might expect the charge degrees of freedom of α Ce to be de-

scribable in terms of itinerant quasiparticles with a large effective mass, a view that is supported by recent optical data [15]. Itinerant quasiparticles are preferable from an energetic standpoint at low temperatures, but the quasi-localized $4f$ electrons of the γ phase will be favored on entropic grounds at elevated temperatures [5, 14].

A magnetic field forms a useful probe of the phenomena discussed above. Based on the absolute size of χ in γ Ce and the large fall in χ at the volume collapse [10, 11], an applied field will chiefly affect the energy and entropy of the quasi-localized $4f$ electrons present in γ Ce; it will have a much smaller effect on the *spd* conduction electrons in γ Ce and on the itinerant quasiparticles of α Ce [14, 15]. In this paper, we have therefore applied steady magnetic fields of up to 27 T and pulsed fields of up to 57 T to samples of polycrystalline $\text{Ce}_{0.8}\text{La}_{0.1}\text{Th}_{0.1}$. We find that the field B suppresses the $\gamma - \alpha$ transition temperature, $T_{\gamma\alpha}$, so that it extrapolates to zero at a field $B_{\gamma\alpha}(T \rightarrow 0) \approx 56$ T. This result, and the variation of $T_{\gamma\alpha}$ with B , are in agreement with a simple model of the volume collapse based on entropy arguments [14].

There are two reasons to choose $\text{Ce}_{0.8}\text{La}_{0.1}\text{Th}_{0.1}$ rather than pure Ce for such a study. First, the Th content of the alloy completely suppresses the dhcp β phase [16, 17, 18]. By contrast, in pure Ce at ambient pressure the metastable β phase (lifetime $\sim 10^4$ years) is a considerable complication [2]. Successive thermal cyclings of pure Ce lead to “contamination” of the α phase with varying amounts of β Ce [2, 11]. Moreover, β Ce has a large susceptibility, and the presence of even tiny amounts in the α phase sorely hinders magnetic measurements [2, 11]. Second, the La content of the alloy leads to a $T_{\gamma\alpha}(B = 0)$ that is significantly lower than that in pure Ce [16, 17], enabling the transition to be completely suppressed by available magnetic fields.

The samples are prepared by arc melting the pure metals in an argon atmosphere. The Ce and La used are 99.99% pure and the Th purity is 99.9% (suppliers’ fig-

ures). The raw materials are melted together, and then flipped and remelted a number of times to ensure sample homogeneity. The uniformity of the composition is further ensured by annealing in vacuum for 8 days at 460°C. Samples for the resistivity and magnetization measurements are spark cut from the resulting ingots. Electrical contacts are made using 50 μm Pt wires attached using spot welding. Resistance data are recorded in either a Quantum Design PPMS (data from 0 – 14 T) or a variable-temperature probe within a 30 T Bitter magnet at NHMFL Tallahassee (data from 0 – 27 T); in both cases, the temperature sensor is a calibrated Cernox resistor close to the sample. The sample resistance is measured using either a Linear Research LR700 bridge (Bitter magnet experiments) or the resistivity option of the PPMS; the two methods are in good agreement.

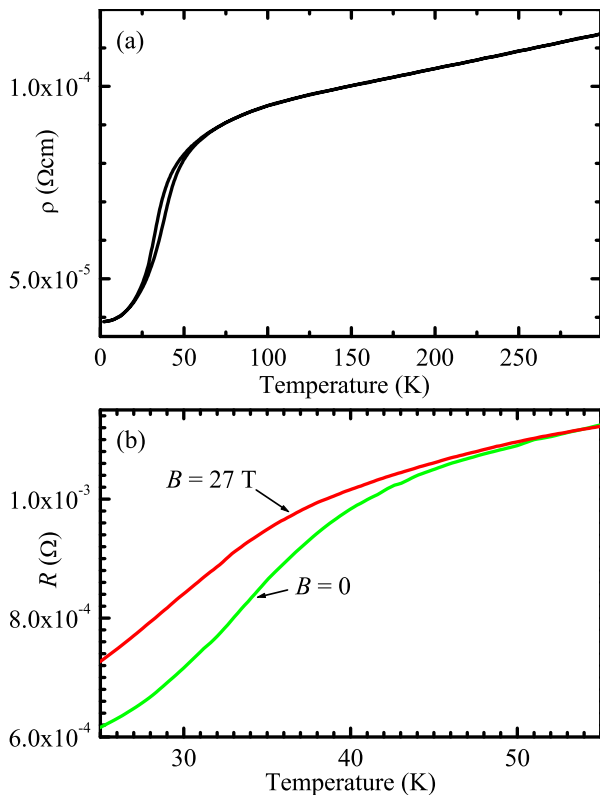


FIG. 1: (a) Resistivity of $\text{Ce}_{0.8}\text{La}_{0.1}\text{Th}_{0.1}$ as a function of temperature at zero applied magnetic field. The data are recorded by sweeping the temperature at $\sim 1 \text{ Kmin}^{-1}$ from 300 K to 2 K and then back to 300 K. Note the hysteresis between down- and up-sweeps of the temperature close to the transition. (b) Resistance of a $\text{Ce}_{0.8}\text{La}_{0.1}\text{Th}_{0.1}$ sample versus temperature at applied magnetic fields B of 0 and 27 T. In each case, the sample is being warmed above 200 K and then cooled at $\sim 1 \text{ Kmin}^{-1}$ in the stated fixed field.

Fig. 1(a) shows typical resistivity versus temperature data with the sample in zero applied magnetic field. The $\gamma - \alpha$ transition is visible as a reduction in resistivity over a broad range of temperature that starts at about 60 K; note that in agreement with previous mea-

surements of $\text{Ce}_{0.8}\text{La}_{0.1}\text{Th}_{0.1}$ [17], there is hysteresis between data recorded as the temperature falls and those taken as it rises. Although the hysteresis is only clearly visible close to the $\gamma - \alpha$ transition, there is a large amount of irreversibility and dissipation involved in the volume collapse; in common with other studies of Ce alloys [16, 17], it is necessary to raise the sample temperature to above 200 K before each sweep of the temperature down through the transition to obtain consistent results. In what follows, we concentrate on data acquired as the temperature *falls* from 200 K through $T_{\gamma\alpha}$, so that the transition is always from γ to α .

Various zero-field thermodynamic measurements of the $\text{Ce}_{0.8}\text{La}_{0.1}\text{Th}_{0.1}$ samples [19] show that the $\gamma - \alpha$ transition occurs at $T_{\gamma\alpha}(0) = 47 \pm 1 \text{ K}$. The corresponding point in the resistance data is extracted using a variety of methods (*e.g.* intersection of extrapolations from above and below the transition, fitting of dR/dT to a Gaussian); in general, these methods give values of $T_{\gamma\alpha}(0)$ within 1 K of each other and within 1 K of the zero-field thermodynamic measurements.

Fig. 1(b) shows the effect of applied magnetic field B on the $\gamma - \alpha$ transition; it is clear that the fall in resistance is displaced to lower temperatures. Correspondingly, the fitting and extrapolation procedures mentioned above give a transition temperature of $T_{\gamma\alpha}(27 \text{ T}) = 40.9 \pm 0.7 \text{ K}$. Data acquired at several other fields illustrate a similar trend; *i.e.* the transition temperature is suppressed by increasing applied field.

Magnetization measurements provide a complementary thermodynamic method for examining the field dependence of the $\gamma - \alpha$ transition. Fig. 2 shows examples of such data recorded at fixed temperatures using an extraction magnetometer inside a 57 T pulsed magnet at NHMFL Los Alamos [20]; before each measurement, the sample is heated to 200 K and then cooled slowly ($\sim 1 \text{ Kmin}^{-1}$) to the required temperature.

Data for temperatures above $T_{\gamma\alpha}$ (*e.g.* the $T = 50 \text{ K}$ data shown in Fig. 2) show a relatively large susceptibility $\chi = dM/dH$, in agreement with expectations for the γ phase [10, 11, 16]. At very low temperatures, unambiguously in the α phase (*e.g.* the $T = 1.5 \text{ K}$ data in Fig. 2), the magnetization increases more slowly, consistent with the small χ observed by others [10, 16]. However, at intermediate temperatures (see the $T = 35 \text{ K}$ data in Fig. 2), there is a distinct “elbow” or change in slope, consistent with a transition from a large χ (at high fields) to a smaller χ (at low fields). We associate this change in χ with a field-induced phase change from γ (high fields) to α (low fields); note that the data shown are downsweeps of the field. The field position of the transition is taken to be the intersection of linear extrapolations of the low- and high-field gradients; in this way, transition fields $B_{\gamma\alpha}(T)$ can be extracted from magnetization data at a number of fixed temperatures T .

The transition temperatures $T_{\gamma\alpha}(B)$ from the fixed-field resistivity measurements and the transition fields $B_{\gamma\alpha}(T)$ obtained from the fixed-temperature magnetiza-

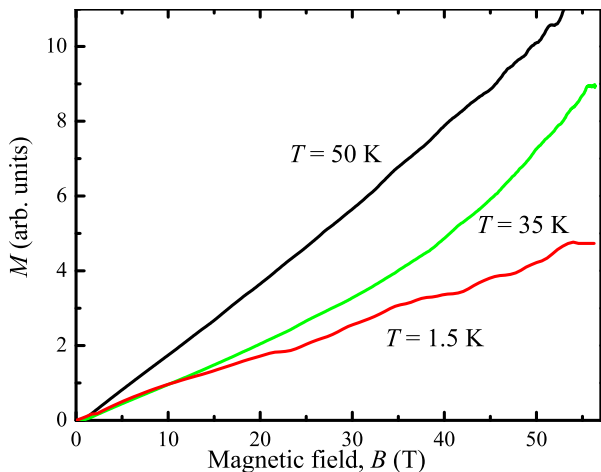


FIG. 2: Examples of pulsed-field magnetization data for a $\text{Ce}_{0.8}\text{La}_{0.1}\text{Th}_{0.1}$ sample at fixed temperatures T . Data corresponding to downsweeps of the magnetic field are shown for $T = 1.5, 35$ and 50 K. Before each shot of the pulsed magnet the sample is warmed to above 200 K and then cooled at $\sim 1 \text{ Kmin}^{-1}$ to the required temperature.

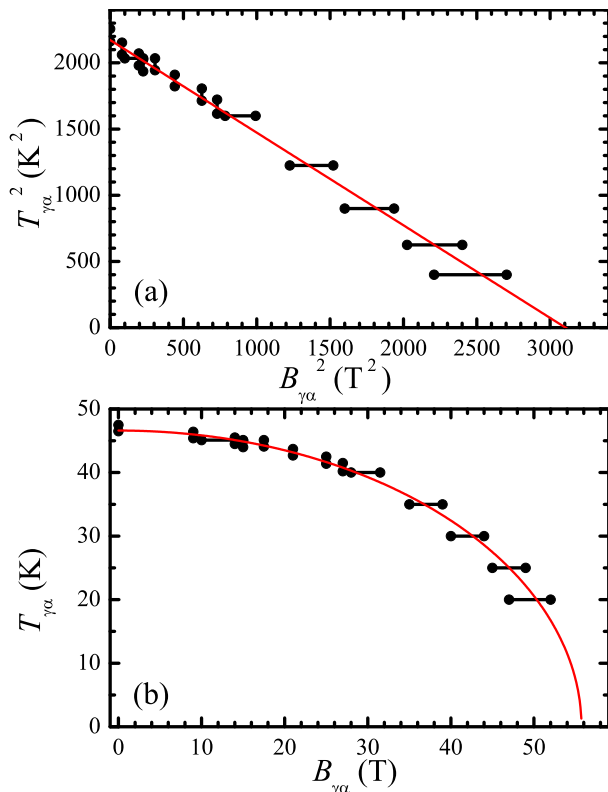


FIG. 3: Values of $B_{\gamma\alpha}(T)$ from the magnetization experiments at fixed temperature T (horizontal error bars) and values of $T_{\gamma\alpha}(B)$ from resistivity experiments at fixed field B (vertical error bars) plotted as T^2 versus B^2 (a) and in linear units (b). The line in (a) and the curve in (b) represent Eq. 2 with $B_{\gamma\alpha}(T \rightarrow 0) = 56 \text{ T}$ and $T_{\gamma\alpha}(B = 0) = 46.6 \text{ K}$.

tion experiments are summarized in Figs. 3(a) and (b). Data from the two techniques may be distinguished as follows; owing to the width of the transition, the $B_{\gamma\alpha}(T)$ points from the magnetization experiments have quite a large field uncertainty [21]. These data are therefore plotted as horizontal error bars. On the other hand, the $T_{\gamma\alpha}(B)$ values from resistivity data possess a relatively large temperature uncertainty, so that they are represented by vertical error bars. In spite of the differences between the measurement techniques, there is reasonable agreement between the two sets of data shown in Fig. 3. Note also that the data lie on a straight line when plotted in the form $B_{\gamma\alpha}^2$ versus $T_{\gamma\alpha}^2$ (Fig. 3(a)).

In order to understand the variation of the γ to α transition with field and temperature, we turn to the two-phase magnetic entropy model of Dzero *et al.* [14]. This is based on the premise that the low-temperature phase possesses an energy scale characterized by an effective Kondo temperature $T_{K\alpha}$ that is much larger than the corresponding energy scale for the high-temperature phase, $T_{K\gamma}$, *i.e.* $T_{K\alpha} \gg T_{K\gamma}$. This view is supported by variety of experiments that suggest $k_B T_{K\alpha} \sim 80 - 170 \text{ meV}$ and $k_B T_{K\gamma} \sim 5 - 8 \text{ meV}$ (see Refs. [5, 11, 12, 13, 14] and references therein). The large value of $T_{K\alpha}$ means that the free energy $F_\alpha(B, T)$ of the α phase will vary only slowly with B . By contrast the quasi-localized $4f$ electrons of the γ phase will couple strongly to the applied field, producing a large negative contribution to the γ phase's free energy, $F_\gamma(B, T)$. This distinction is emphasized [14] by writing $F_\gamma = E_0 - TS(B, T)$, where E_0 indicates the contribution of the itinerant *spd* electrons and $S(B, T)$ is the entropy associated with the $4f$ multiplet of angular momentum J , Landé g -factor g_J ;

$$TS(B, T) = -T \log_e \left(\sum_{m_J = -J}^J \exp\left[-\frac{g_J \mu_B B m_J}{T}\right] \right). \quad (1)$$

The phase boundary is defined by the equivalence of the free energies, $F_\gamma(B, T) = F_\alpha(B, T)$. Owing to the fact that both $F_\alpha(B, T)$ and E_0 will vary relatively slowly with B and T compared to $TS(B, T)$, the approximate condition for the phase boundary becomes $TS(B, T) \approx \text{constant}$. With this constraint, straightforward manipulation of Eq. 1 (see Ref. [14]) yields the following equation relating the fields and temperatures on the $\gamma - \alpha$ phase boundary;

$$\left(\frac{B_{\gamma\alpha}}{B_{\gamma\alpha}(T \rightarrow 0)} \right)^2 + \left(\frac{T_{\gamma\alpha}}{T_{\gamma\alpha}(B = 0)} \right)^2 \approx 1, \quad (2)$$

i.e. a plot of $B_{\gamma\alpha}^2$ versus $T_{\gamma\alpha}^2$ should yield a straight line.

The straight line in Fig. 3(a) is a fit of the data to Eq. 2 with $B_{\gamma\alpha}(T \rightarrow 0)$ and $T_{\gamma\alpha}(B = 0)$ as adjustable parameters. The values obtained were $B_{\gamma\alpha}(T \rightarrow 0) = 56 \pm 1 \text{ T}$ [21] and $T_{\gamma\alpha}(B = 0) = 46.6 \pm 0.5 \text{ K}$. A consistency check of these values can be obtained by again setting $TS(B, T)$ equal to a constant and examining Eq. 1

in the limits $B = 0$ and $T \rightarrow 0$; this produces

$$\frac{k_B T_{\gamma\alpha}(B = 0)}{\mu_B B_{\gamma\alpha}(T \rightarrow 0)} = \frac{g_J J}{\log_e(2J + 1)} \approx 1.20, \quad (3)$$

where we have inserted the known values [10, 11] $J = \frac{5}{2}$ and $g_J = \frac{6}{7}$ for the quasi-localized f electrons of γ Ce. Using the fit parameters derived from Fig. 3, the experimental ratio $k_B T_{\gamma\alpha}(B = 0)/\mu_B B_{\gamma\alpha}(T \rightarrow 0)$ is 1.24, within a few percent of the prediction of Eq. 3.

It is interesting to note that a rather simple model [14] produces an internally self-consistent description of these data. The model, in effect, neglects the field and temperature dependences of *both* the *spd* electrons of the γ phase, and the itinerant, hybridized *spdf* state [15] of the α phase, treating only the free energy contributed by the well-defined moments present in the γ phase. Hence, the success of the model suggests that the $\gamma - \alpha$ transition is driven mainly by the fact that entropy considerations favor f electrons that are effectively localized at high temperatures and fields (and, one might add, at low pressures [5]). The delocalization of the f electrons manifested as the itinerant quasiparticle behavior [15] of the α phase is energetically favorable from zero-point-energy considerations, but it is costly on entropic grounds. Thus, α Ce is stable at low temperatures and fields (and at high pressures). Finally, we remark that it has been argued on the basis of a qualitative assessment of phonon spectra that the entropy of the $4f$ moments plays a dominant role in determining the structural phase of $\text{Ce}_{0.9}\text{Th}_{0.1}$ [18]. The success of the magnetic entropy model in the current work adds a *quantitative* justification to this argument.

In summary, we have measured the $\gamma - \alpha$ transition in $\text{Ce}_{0.8}\text{La}_{0.1}\text{Th}_{0.1}$ as a function of applied magnetic field using both resistivity and magnetization. The transition temperature is suppressed by increasing magnetic field, extrapolating to absolute zero at around 56 T. The magnetic field-temperature phase boundary is adequately fitted by a simple model [14] of the field and temperature dependence of the entropy of the localized f -electron moments in the γ phase. This suggests that the volume collapse in Ce and its alloys is primarily driven by entropic considerations. Many substances undergo structural phase transitions which are thought to involve f electrons changing from “localized” to itinerant behavior (*e.g.* Plutonium [22]). On the basis of the work reported in the present paper, it seems likely that the application of high magnetic fields to such substances will yield valuable information about the role of the f electron system in stabilizing the various structural phases.

This work is supported by the U.S. Department of Energy (DOE) under Grant No. 1drd-dr 20030084 “Quasiparticles and Phase Transitions in High Magnetic Fields: Critical Tests of Our Understanding of Plutonium” and by the National Science Foundation (NSF) (grant DMR-0433560). It is also sponsored by the National Nuclear Security Administration under the Stewardship Science Academic Alliances program through DOE grant DE-FG03-03NA00066. Part of this work was carried out at the National High Magnetic Field Laboratory, which is supported by NSF, the State of Florida and DOE. We thank Lev Gor’kov, Alex Lacerda and Peter Littlewood for enthusiastic and helpful comments and are grateful to Stan Tozer for experimental assistance.

-
- [1] A.W. Lawson and Ting-Yuan Tang, Phys. Rev. **76**, 301 (1949).
- [2] D.C. Koskenmaki and K.A. Gschneider, in *Handbook on the Physics and Chemistry of Rare Earths*, eds K.A. Gschneider and L. Eyring (North Holland, Amsterdam, 1978), p337.
- [3] D. Malterre, M. Grioni and Y. Baer, Adv. Phys. **45**, 299 (1996).
- [4] A.V. Nikolaev and K.H. Michel, Phys. Rev. B **66**, 054103 (2002).
- [5] J. Laegsgaard and A. Svane, Phys. Rev. B **59**, 3450 (1999).
- [6] K. Held, A.K. McMahan and R.T. Scalettar, Phys. Rev. Lett. **87**, 276404 (2001).
- [7] B. Johansson, Philos. Mag **30**, 469 (1974).
- [8] A. Svane, Phys. Rev. B **53**, 4275 (1996).
- [9] B. Johansson, I.A. Abrikosov, M. Aldén, A.V. Ruban and H.L. Skriver, Phys. Rev. Lett. **74**, 2335 (1995).
- [10] D.C. Koskimaki and K.A. Gschneider, Phys. Rev. B **11**, 4463 (1975).
- [11] A.P. Murani, Z.A. Bowden, A.D. Taylor, R. Osborn and W.G. Marshall, Phys. Rev. B **48**, 13981 (1993).
- [12] L.Z. Liu, J.W. Allen, O. Gunnarsson, N.E. Christensen and O.K. Andersen, Phys. Rev. B **45**, 8934 (1992).
- [13] J.W. Allen and L.Z. Liu, Phys. Rev. B **46**, 5047 (1992).
- [14] M.O. Dzero, L.P. Gor’kov and A.K. Zvezdin, J. Phys.: Condens. Matter **12**, L711 (2000).
- [15] J.W. van der Eb., A.B. Kuz’menko and D. van der Marel, Phys. Rev. Lett. **86**, 3407 (2001).
- [16] B.H. Grier, R.D. Parks, S.M. Shapiro and C.F. Majkrzak, Phys. Rev. B **24**, 6242 (1981).
- [17] J.D. Thompson, Z. Fisk, J.M. Lawrence, J.L. Smith and R.M. Martin, Phys. Rev. Lett. **50**, 1081 (1983).
- [18] M.E. Manley, R.J. McQueeney, B. Fultz, T. Swan-Wood, O. Delaire, E.A. Goremychkin, J.C. Cooley, W.L. Hults, J.C. Lashley, R. Osborn and J.L. Smith, Phys. Rev. B **67**, 014103 (2003).
- [19] J.C. Lashley, unpublished data (2003).
- [20] J. Singleton, C.H. Mielke, A. Migliori, G.S. Boebinger and A. H. Lacerda, Physica B **346-347**, 614 (2004).
- [21] At temperatures below ~ 15 K, the transition field $B_{\gamma\alpha}$ rapidly approaches the upper field limit (57 T) of the magnet used. Owing to the broadness of the $\gamma - \alpha$ transition, this limitation prevents us from assigning $B_{\gamma\alpha}$ values with any confidence for temperatures of 15 K and below.

- [22] J.C. Lashley, J. Singleton, A. Migliori, J.B. Betts, R.A. Fisher, J.L. Smith and R.J. McQueeney, Phys. Rev. Lett. **91**, 205901 (2003).